Transactions of the TSME (2016) Vol. 4, No. 2, 192-201
Journal of Research and Applications in Mechanical Engineering

ISSN 2229-2152 print
DOI: 10.14456/jrame.2016.20

Research Article

NUMERICAL THERMAL PERFORMANCE STUDY IN A HEAT EXCHANGER TUBE WITH DISCRETE V-RIBS

N. Koolnapadol[1]
S. Skullong [2,*]
T. Sutthanonkul [3]
P. Loraphong[3]
T. Sooksin[3]
[1] Department of Automotive Mechanical Engineering, Faculty of Industrial Technology, Rajabhat Rajanagarindra University, Chachoengsao 24000, Thailand
[2] Energy Systems Research Group, Department of Mechanical Engineering, Faculty of Engineering at Sriracha, Kasetsart University Sriracha Campus, Chonburi 20230, Thailand
[3] Department of Mechanical Engineering, Faculty of Engineering, King Mongkut's Institute of Technology Ladkrabang, Bangkok 10520, Thailand

ABSTRACT:
The paper presents a numerical investigation on heat transfer enhancement in a heat exchanger tube fitted with discrete V-ribs by calculating a three dimensional, steady turbulent tube flow model. The six pairs of discrete V-shaped ribs mounted around the tube circumference are used to produce counter-rotating vortices inside the tube that can convey the colder fluid in the core flow to the heated-wall region. The test fluid is water having the flow rate in terms of Reynolds number from 3000 to 25,000. The rib parameters are the attack angle of 45º, two relative rib lengths (L/D=0.2 and 0.3), four pitch ratios (PR=P/D= 0.24, 0.32, 0.48 and 0.64) and a single relative V-rib height (BR=e/D= 0.02). The computation reveals that the tube with circumferential discrete V-ribs provides considerably higher thermal performance than the smooth tube in the range of 1.26 - 2.14. The maximum thermal performance of 2.14 is found for using PR=0.24, L/D=0.3 at Re=3000.

Keywords: *Heat transfer; Numerical analysis; Discrete V-ribs; Turbulent flow*

1. INTRODUCTION

Heat transfer enhancement is significant and needed in engineering applications of thermal equipment such as dryer, oven, heat exchanger, distillation, freezer, condenser and engine. At present, most of industries use a heat exchanger in the process of manufacturing. Therefore, improving the heat exchanger is necessary to obtain higher performance since it will help save energy and decrease the cost of operation. The most commonly technique found in literature is in the passive technique group such as dimpled tubes, grooved tubes, ribbed tubes, corrugated tubes, and various tube inserts. The techniques mentioned earlier provide the considerable increase in the heat transfer rate of cooling/heating systems because the tube surface roughness can generate the transverse/longitudinal vortex flow, apart from the increase in turbulent intensity. In addition, the vortex flow and the surface roughness shapes can interrupt or destroy thermal and velocity boundary layers of the tube flow leading to higher heat transfer rate in tubes. However, the requirement of general heat exchanger design needs the longitudinal vortex flow rather than the transverse vortex flow [1,2].

Li et al. [3] studied experimentally and numerically thermal characteristics in the heat exchanger tube with discrete double inclined ribs (DDIR). They used water as working fluid with Reynolds numbers from 15,000 to 60,000 and found that the heat transfer in the DDIR tube was enhanced around 100-120% compared with the plain tube while the pressure drop increased at about 170-250%. The highest thermal performance of 1.56 was for the DDIR tube with rib height of 0.75 mm, number of circumferential ribs = 12, and rib pitch of 6 mm.

* Corresponding author: S. Skullong
E-mail address: sfengsps@src.ku.ac.th

Bilen et al. [4] experimentally investigated on turbulent flow and heat transfer in a grooved tube with three geometric groove shapes (circular, trapezoidal and rectangular) and found that the heat transfer enhancement was obtained up to 63% for circular groove, 58% for trapezoidal groove and 47% for rectangular groove, compared to the smooth tube. Lu et al. [5] measured and analyzed the transition and turbulent convective heat transfer of molten salt in a spirally grooved tube with four relative groove height (e/D=0.0238, 0.0306, 0.0381 and 0.0475) and reported that the increment of e/D remarkably enhanced heat transfer in the grooved tube. Tang et al. [6] performed a numerical study of various groove configurations including P-type grooves, V-type grooves and W-type grooves on turbulent heat transfer in a channel and pointed that the heat transfer and friction loss for the P-type grooves was enhanced by 45.8–65.4% and 95.1–114.8%, respectively, compared to smooth channel. Zheng et al. [7] conducted a numerical analysis on the thermal-hydraulic performance in a rib-grooved heat exchanger tube and showed that the heat transfer and friction factor of the rib-grooved tube was improved around 1.58-2.46 and 1.82-5.03 times above the smooth tube, respectively.

Numerical analyses of flow pattern and heat transfer in an internally ribbed heat exchanger tube with parallel type ribs (P-type ribs) and V-shape type ribs (V-type ribs) were carried out by Zheng et al. [8]. Their results showed that the heat transfer and friction loss in the V-type ribbed tubes are about 57-76% and 86-94% higher than those in the P-type ribbed tube, respectively. Zheng et al. [9] conducted a numerical investigation on heat transfer enhancement in a novel internally grooved tube by generating longitudinal swirl flows with multi-vortexes and indicated that the maximum overall thermal-hydraulic performance based on the same pumping power (PEC= 1.52) was achieved with the groove inclination of 30° at the lowest Reynolds number. Zheng et al. [10] again numerically investigated the convective heat transfer and turbulent flow in a heat exchanger tube with discrete inclined grooves. The results showed that the Nusselt number and friction factor are enhanced by a factor of approximately 1.23-2.17 and 1.02-3.75 over the smooth tube, respectively.

In the present work, the computation of turbulent tube flow through discrete V-ribs mounted on the tube wall is performed to investigate the optimum heat transfer enhancement including the turbulent flow structure for Re ranging from 3000 to 25,000.

2. TUBE FLOW CONFIGURATION

The tube flow model in this research is expected to attain a periodically fully developed flow where the velocity field repeats itself from one cell/module to another. In the flow model, the water flows into a tube having the inner diameter, D = 25 mm, T_{in} = 300 K. Ribs in the present work can be formed by extruding the tube surface to be a capsule-like shape with the number of circumferential ribs of 12 (θ = 30°) as depicted in Fig. 1. Therefore, there are 6 pairs of discrete V-ribs. The rib characteristics include the rib width, W= 2 mm; the attack angle, α = 45°; a single ratio of rib height to tube diameter, called blockage ratio, BR=e/D=0.02; four ratios of axial distance of adjacent V-ribs to tube diameter, called pitch ratio, PR=P/D=0.24, 0.32, 0.48, 0.64 and two lengths of the rib element, L/D = 0.2 and 0.3. Due to symmetry around its axis, only one-twelfth of the tube flow is employed as a computational domain as seen in Fig. 2.

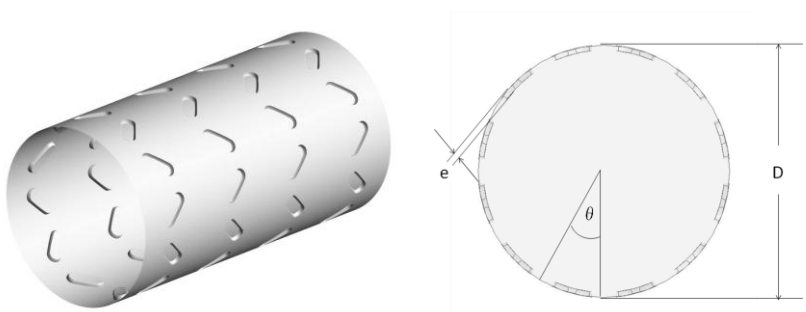

Fig. 1. Ribbed-tube geometry and its axis-symmetry.

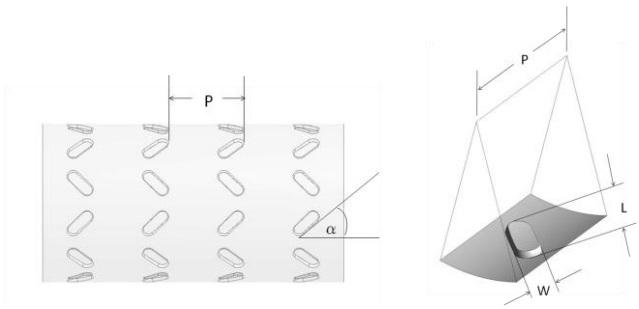

Fig. 1. Ribbed-tube geometry and its axis-symmetry (Continued).

Fig. 2. Grids used for computational domain.

3. COMPUTATIONAL DETAILS

3.1 Governing equations and turbulence modeling

The flow is assumed to be a steady three-dimensional turbulent, incompressible flow with constant fluid properties. The body forces, viscous dissipation and radiation of heat transfer are neglected. By assumptions above, the numerical model is governed by the Reynolds averaged Navier-Stokes (RANS) equations and the energy equation. These equations in the Cartesian tensor system can be written as follows:
Continuity equation:

$$\frac{\partial}{\partial x_i}\left(\rho u_i\right)=0 \tag{1}$$

Momentum equation:

$$\frac{\partial}{\partial x_j}\left(\rho u_i u_j\right)=-\frac{\partial p}{\partial x_i}+\frac{\partial}{\partial x_j}\left[\mu\left(\frac{\partial u_i}{\partial x_j}-\rho\overline{u_i' u_j'}\right)\right] \tag{2}$$

in which ρ is fluid density, and u_i is mean velocity component in direction x_i, p is pressure, μ is dynamic viscosity, and u' is a fluctuating velocity component. Repeated indices indicate summation from one to three for 3D flow problems.
Energy equation:

$$\frac{\partial}{\partial x_i}(\rho u_i T) = \frac{\partial}{\partial x_j}\left((\Gamma + \Gamma_t)\frac{\partial T}{\partial x_j}\right) \tag{3}$$

where Γ and Γ_t are molecular thermal diffusivity and turbulent thermal diffusivity, respectively and are given by

$$\Gamma = \frac{\mu}{\mathrm{Pr}}, \text{ and } \Gamma_t = \frac{\mu_t}{\mathrm{Pr}_t} \tag{4}$$

The RANS equation needs that the Reynolds stresses, $-\rho\overline{u_i' u_j'}$ appearing in (2) requires to be modeled. The Boussinesq hypothesis relates the Reynolds stresses to the mean velocity gradients as seen in (5) below:

$$-\rho\overline{u_i' u_j'} = \mu_t\left(\frac{\partial u_i}{\partial u_j} + \frac{\partial u_j}{\partial u_i}\right) - \frac{2}{3}\left(\rho k + \mu_t \frac{\partial u_i}{\partial x_i}\right)\delta_{ij} \tag{5}$$

where k is turbulent kinetic energy, defined by $k = 1/2 \cdot \overline{u_i' u_i'}$ and δ_{ij} is a Kronecker delta. The merit for using Boussinesq approach is the relatively low computational cost for calculating the turbulent dynamic viscosity, μ_t given as $\mu_t = \rho C_\mu k^2 / \varepsilon$. The Realizable k-ε model, an improvement over the standard k-ε model, was used in the current research.

The QUICK numerical scheme was employed for discretizing all the governing equations and the discretized equations were solved based on the finite volume method [11]. The SIMPLE algorithm was used for pressure-velocity coupling. The Realizable k-ε model was utilized for closure of the equations. No slip and constant temperature for rib surface and tube walls were set as boundary conditions. The fully-developed periodic flow condition was applied to the inlet and outlet sections while due to axis-symmetry one-twelfth tube section was utilized as shown in Fig. 1 and 2. The solutions were converged when the residual values were less than 10^{-6} for all variables but less than 10^{-9} for the energy equation.

There are four parameters of interest included Reynolds number (Re), friction factor (*f*), Nusselt number (Nu) and thermal enhancement factor (TEF). The Re is defined as

$$\mathrm{Re} = \frac{\rho \bar{u} D}{\mu} \tag{6}$$

The *f* is evaluated from pressure drop, Δp across the tube length, P as

$$f = \frac{(\Delta p / P)D}{(1/2)\rho \bar{u}^2} \tag{7}$$

The local Nu is calculated by

$$Nu_x = \frac{h_x D}{\lambda} \tag{8}$$

where λ is fluid thermal conductivity.

The area-averaged Nu is obtained from

$$Nu = \frac{1}{A}\int Nu_x \partial A \tag{9}$$

The thermal enhancement factor (TEF) defined as the ratio of the dimensionless heat transfer coefficient of the ribbed tube (Nu) to that of the smooth tube (Nu_0) at an equal pumping power proposed by Webb and Kim [12] is adopted. It is calculated based on the following formula:

$$\mathrm{TEF} = \frac{\mathrm{Nu}/\mathrm{Nu}_0}{(f/f_0)^{1/3}} \tag{10}$$

in which Nu_0 and f_0 are Nusselt number and friction factor for the smooth tube, respectively.

4. RESULTS AND DISCUSSION

4.1 Grid independence

For finding grid independence solution, we use four sets of different grid sizes. The average Nusselt numbers and friction factors for the four sets of the grids at Reynolds number of 5000 are listed in Table 1. The relative difference for the simulated Nu using a grid size of 207034 and 402127 elements is 0.23%, with a relative difference for the computed *f* of 0.41%. Therefore, the grid is considered to be sufficiently fine for the simulation. The grid size of about 200,000 elements was used in the present simulation.

Table 1: Grid independence test at Re = 5000

Grid size	Nu	*f*
53261	84.3206	0.06747
107795	84.2803	0.06928
207034	83.8292	0.06968
402127	83.6358	0.06996

For validate the flow model, the numerical results are compared with the experimental results taken from [3] for a similar flow condition. The comparison of numerical Nu and *f* for Re ranging from 10,000 to 60,000 with measured data [3] is presented in Fig. 3(a) and (b), respectively. Also, numerical Nu and *f* values obtained from using the standard and RNG k-ε turbulence models are included in the figure for comparison. In the figure, numerical results are in reasonably good agreement with experimental results for both Nusselt number and friction factor, especially for the Realizable k-ε model. Thus, the Realizable k-ε model is the best choice for this flow model and the maximum error between the computational and experimental data are 7% for Nu and 15% for *f* in the range of Re = 3000-25000. Thus, the numerical model in the current study can be judged to be reliable.

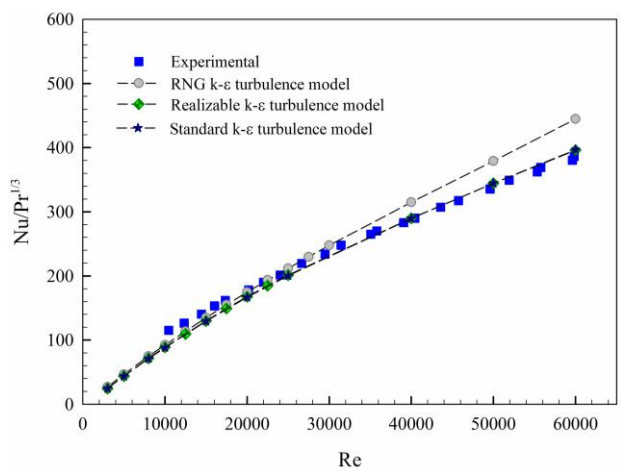

(a)

Fig. 3. Validation of numerical (a) Nu and (b) *f* with experimental data.

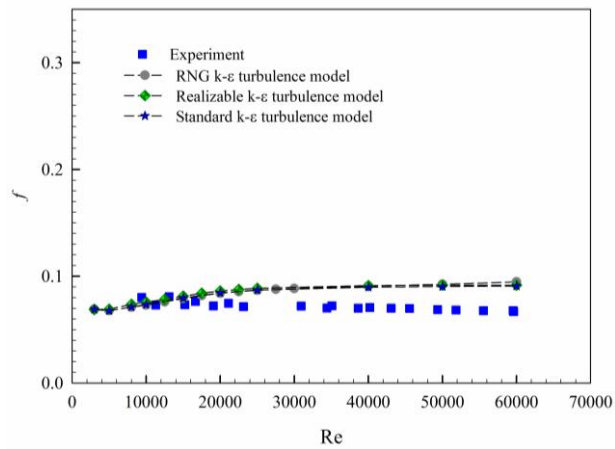

(b)

Fig. 3. Validation of numerical (a) Nu and (b) *f* with experimental data (continued).

4.2 Flow structure

Figure 4(a) and (b) shows the streamlines in transverse planes and longitudinal streamlines at Re=8000, respectively. As seen in this figure six pairs of counter-rotating vortices appear and are created by the discrete V-ribs. Fig. 4(b) shows the small vortices occur upstream and downstream the V-ribs called front and rear vortices while the rear vortex has a substantial effect on the heat transfer at tube surface.

Figure 5 depicts the temperature contours in a transverse plane at the mid-rib location for PR=0.48, L/D=0.2, Re=8000. It is noted that the cold fluid core is induced to the near-wall hot fluid region. The colder fluid area near the tube wall can be seen where the common-flow-down vortices appear. The high temperature gradient at the surface contributes to enhance the heat transfer rate.

The plot of local Nusselt number contours on the ribbed tube at PR=0.48, L/D =0.2, Re=8000 is displayed in Fig. 6. In the figure, it is visible that peak Nu values are found on the rib surface area, especially on the rib front. Also, higher Nu values can be seen on the tube surface area downstream of the rib. Lower Nu values are observed on the vicinity of the rib except for the front rib region. It is concluded that the application of the discrete V-ribs can improve the thermal performance of the tube by considering the local Nusselt number area as mentioned earlier. This may be due to higher strength of secondary flow or vortex-induced impingement of six pairs of vortices behind the ribs.

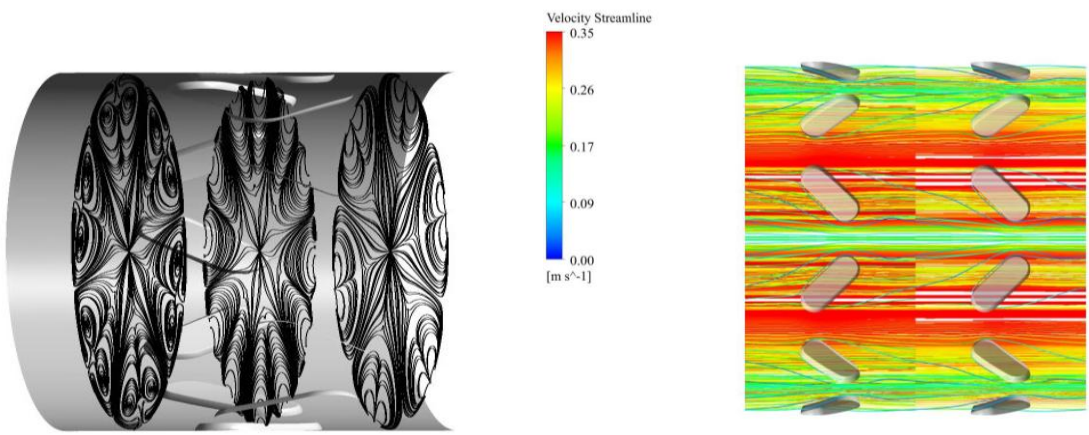

(a) (b)

Fig. 4. (a) Streamlines in 2D and (b) streamlines in 3D views.

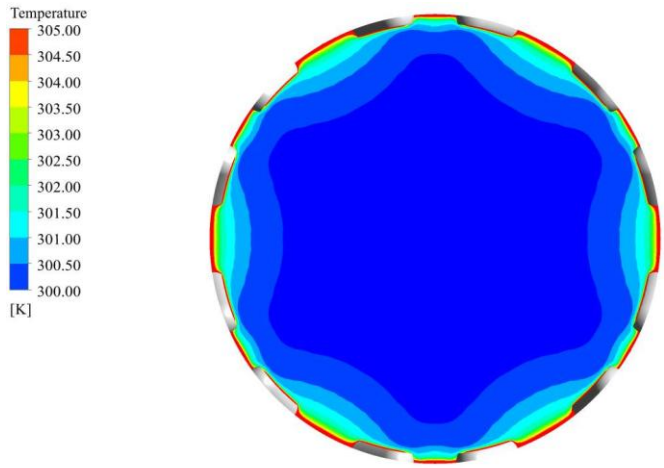

Fig. 5. Temperature contours in transverse plane.

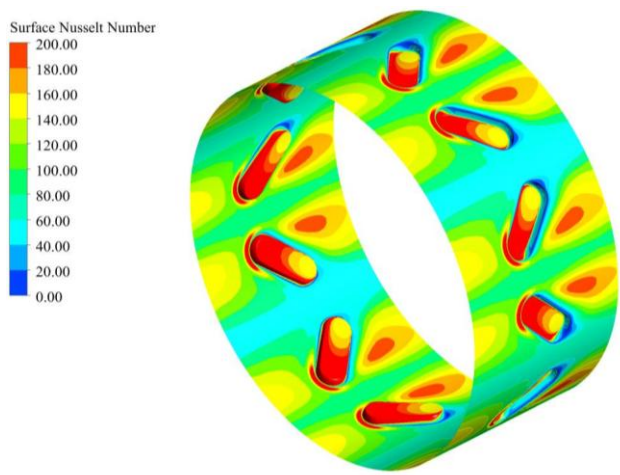

Fig. 6. Local Nusselt number contours.

4.3 Effect of PR and rib length (L/D)

The variations of Nusselt number and friction factor ratios with Reynolds number for different PR and L/D values are depicted in Fig. 7(a) and (b), respectively. Nu/Nu_0 for the ribbed tube is considerably greater than that for the smooth tube. The Nu/Nu_0 mostly decreases slightly with increasing Re except for PR=0.24 that increases slightly at the beginning for further Re. However, Nu/Nu_0 increases significantly with the rise of L/D but with decreasing PR. The maximum Nu/Nu_0 is approximately 2.9 at PR=0.24, L/D=0.3 and Re=8000.

The heat transfer enhancement is commonly concerned with higher pressure drop across the tube's length. Figure 7(b) shows that f/f_0 increases considerably with increasing Re and L/D but displays the reversing trend for the rise of PR. The highest f/f_0 is approximately 5.0 times at PR=0.24, L/D =0.3 and Re=25,000.

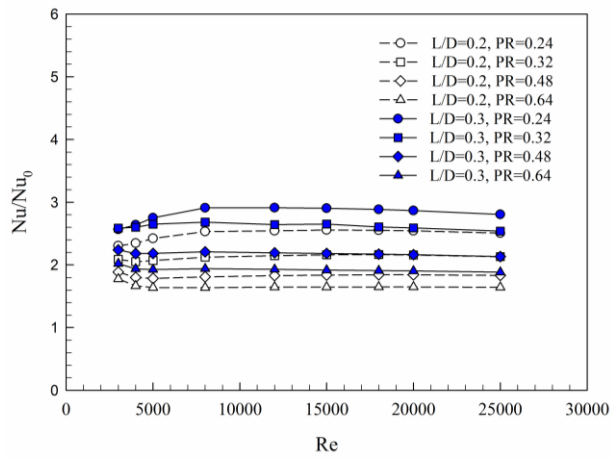

(a)

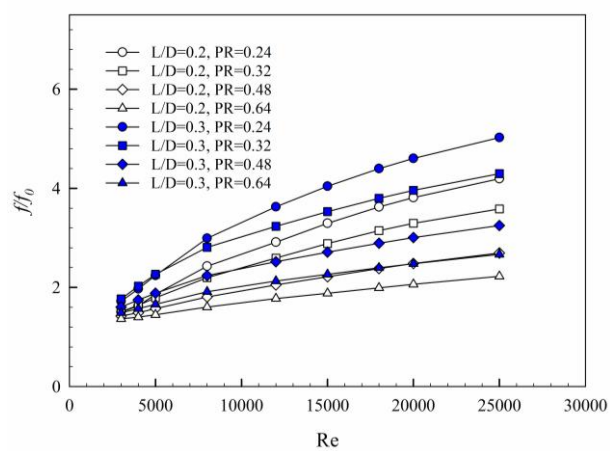

(b)

Fig. 7. Variations of (a) Nu/Nu_0 (b) f/f_0 with Re for varied PR and L/D.

The thermal enhancement factor (TEF) for the water flow into the discrete V-ribbed tube is presented in Fig. 8. In the figure, TEF shows the decreasing trend with the increment of Re and PR while yields the opposite trend for increasing L/D. However, the TEF displays a steep decrease for $3000 < Re < 5000$. The TEF values are found in the range of 1.26 to 2.14. The maximum TEF of about 2.14 is seen at PR=0.24, L/D=0.3 and Re=3000.

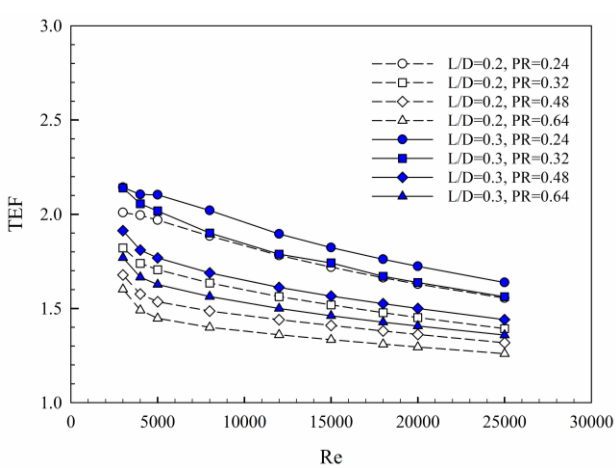

Fig. 8. Variation of TEF with Re for varied PR and L/D.

5. CONCLUSIONS

In the present study, a numerical study on turbulent flow and thermal characteristics in a round tube fitted with discrete V-ribs has been conducted. The numerical results show the six pairs of counter-rotating vortices caused by the six pairs of discrete V-ribs. Those V-ribs that give rise to the six pairs of vortices have a significant effect on the flow structure and the heat transfer rate on the tube surface. It is found that the tube with discrete V-ribs provide higher thermal performance than the smooth tube in the range of 1.26 to 2.14 times. The highest TEF around 2.14 is achieved at PR=0.24, L/D=0.3 and Re=3000.

NOMENCLATURE

A	convention heat transfer area, m^2
BR	blockage ratio (e/D)
D	inner diameter of tube, m
e	rib height, m
f	friction factor
h	convective heat transfer coefficient, W/m^2 K
k	turbulent kinetic energy (TKE), $k = \frac{1}{2} \cdot \overline{u_i' u_i'}$
L	length of rib element, m
Nu	average Nusselt number
P	axial pitch spacing of rib, m
p	static pressure, Pa
Pr	Prandtl number
PR	pitch ratio (P/D)
Re	Reynolds number
T	temperature, K
TEF	thermal enhancement factor
u_i	velocity component in x_i-direction, m/s
$\bar{u}$	mean velocity, m/s
W	rib width, m

Greek letter

μ	dynamic viscosity, kg/m s
Γ	thermal diffusivity
α	attack angle of rib, degree
λ	thermal conductivity of fluid, W/m K
ρ	fluid density, kg/m^3
ε	dissipation rate of TKE, m^2/s^3

Subscripts

in	inlet
0	smooth tube
t	turbulent

REFERENCES

[1] M. Fiebig, Embedded vortices in internal flow: Heat transfer enhancement, Int. J. Heat Fluid Flow, Vol. 16, 1995, pp. 376–388.

[2] M. Fiebig, P. Kallweit, N. Mitra, S. Tiggelbeck, Heat transfer enhancement and drag by longitudinal vortex generators in channel flow, Exp. Therm. Fluid Sci., Vol. 4, 1991, pp.103–114.

[3] X.W. Li, J.A. Meng, Z.Y. Guo, Turbulent flow and heat transfer in discrete double inclined ribs tube, Int. J. Heat Mass Transfer, Vol. 52, 2009, pp. 962–970.

[4] K. Bilen, M. Cetin, H. Gul, T. Balta, The investigation of groove geometry effect on heat transfer for internally grooved tubes, Appl. Therm. Eng., Vol. 29, 2009, pp. 753–761.

[5] J. Lu, X. Sheng, J. Ding, J. Yang, Transition and turbulent convective heat transfer of molten salt in spirally grooved tube, Exp. Therm. Fluid Sci., Vol. 47, 2013, pp. 180–185.
[6] X.-Y. Tang, G. Jiang, G. Cao, Parameters study and analysis of turbulent flow and heat transfer enhancement in narrow channel with discrete grooved structures, Chem. Eng. Res. Des., Vol. 93, 2015, pp. 232–250.
[7] N. Zheng, P. Liu, F. Shan, Z. Liu, W. Liu, Numerical investigations of the thermal-hydraulic performance in a rib-grooved heat exchanger tube based on entropy generation analysis, Appl. Therm. Eng., Vol. 99, 2016, pp. 1071–1085.
[8] N. Zheng, P. Liu, F. Shan, Z. Liu, W. Liu, Effects of rib arrangements on the flow pattern and heat transfer in an internally ribbed heat exchanger tube, Int. J. Therm. Sci., Vol. 101, 2016, pp. 93–105.
[9] N. Zheng, P. Liu, F. Shan, Z. Liu, W. Liu, Heat transfer enhancement in a novel internally grooved tube by generating longitudinal swirl flows with multi-vortexes, Appl. Therm. Eng., Vol. 95, 2016 pp. 421–432.
[10] N. Zheng, P. Liu, F. Shan, Z. Liu, W. Liu, Turbulent flow and heat transfer enhancement in a heat exchanger tube fitted with novel discrete inclined grooves, Int. J. Therm. Sci., Vol. 111, 2017, pp. 289–300.
[11] S.V. Patankar, Numerical Heat Transfer and Fluid Flow, McGraw-Hill, New York, 1980.
[12] R.L.Webb, N.-H. Kim, Principles of Enhanced Heat Transfer, Taylor Francis, New York, NY, USA, 1994.